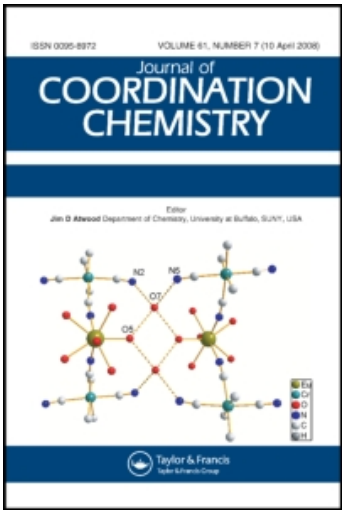

Journal of Coordination Chemistry
Publication details, including instructions for authors and subscription information:
http://www.informaworld.com/smpp/title~content=t713455674

Synthesis, structural characterization, antimicrobial, DNA-binding, and photo-induced DNA cleavage activity of some bio-sensitive Schiff base copper(II) complexes

N. Raman[a]; A. Sakthivel[b]; R. Jeyamurugan[a]
[a] Research Department of Chemistry, VHNSN College, Virudhunagar - 626001, Tamilnadu, India [b] Department of Chemistry, Unnamalai Institute of Technology, Kovilpatti - 628 502, Tamilnadu, India

First published on: 07 December 2010

To cite this Article Raman, N. , Sakthivel, A. and Jeyamurugan, R.(2010) 'Synthesis, structural characterization, antimicrobial, DNA-binding, and photo-induced DNA cleavage activity of some bio-sensitive Schiff base copper(II) complexes', Journal of Coordination Chemistry, 63: 24, 4380 — 4397, First published on: 07 December 2010 (iFirst)
To link to this Article: DOI: 10.1080/00958972.2010.539212
URL: http://dx.doi.org/10.1080/00958972.2010.539212

Journal of Coordination Chemistry
Vol. 63, No. 24, 20 December 2010, 4380–4397

Taylor & Francis
Taylor & Francis Group

Synthesis, structural characterization, antimicrobial, DNA-binding, and photo-induced DNA cleavage activity of some bio-sensitive Schiff base copper(II) complexes

N. RAMAN*†, A. SAKTHIVEL‡ and R. JEYAMURUGAN†

†Research Department of Chemistry, VHNSN College,
Virudhunagar – 626001, Tamilnadu, India
‡Department of Chemistry, Unnamalai Institute of Technology,
Kovilpatti – 628 502, Tamilnadu, India

(*Received 13 May 2010; in final form 12 October 2010*)

Schiff base mixed-ligand copper complexes $[CuL^1(phen)Cl_2]$, $[CuL^1(bipy)Cl_2]$, $[Cu(L^1)_2Cl_2]$, $[Cu(L^2)_2Cl_2]$, $[CuL^2(bipy)Cl_2]$, and $[CuL^2(phen)Cl_2]$ (where L^1 = 4-[3,4-dimethoxy-benzylidene]-1,5-dimethyl-2-phenyl-1,2-dihydro-pyrazole-3-one; L^2 = 4-[3-hydroxy-4-nitro-benzylidene]-1,5-dimethyl-2-phenyl-1,2-dihydro-pyrazole-3-one; phen = 1,10-phenanthroline; and bipy = 2,2′-bipyridine) have been synthesized and characterized. Their DNA-binding properties have been studied by electronic absorption spectra, viscosity, and electrochemical measurements. The absorption spectral and viscosity results suggest that the copper(II) complexes bind to DNA *via* partial intercalation. The addition of DNA resulting in the decrease of the peak current of the copper(II) complexes indicates their interaction. Interaction between the complexes and DNA has also been investigated by submarine gel electrophoresis. The copper complexes cleave supercoiled pUC19 DNA to nicked and linear forms through hydroxyl radical and singlet oxygen in the presence of 3-mercaptopropionic acid as the reducing agent. These copper complexes promote the photocleavage of pUC19 DNA under irradiation at 360 nm. Mechanistic study reveals that singlet oxygen is likely to be the reactive species responsible for the cleavage of plasmid DNA by the synthesized complexes. The *in vitro* antimicrobial study indicates that the metal chelates have higher activity against the bacterial and fungal strains than the free ligands.

Keywords: Copper(II) complexes; Schiff base; DNA-binding; Photocleavage

1. Introduction

"Chemical nuclease" that can bind and cleave DNA and RNA under physiological conditions *via* oxidative and hydrolytic mechanism has attracted considerable interest [1]. Such artificial small molecule catalysts would be valuable tools in biotechnology, nanotechnology, chemotherapeutic approaches, and in the study of nucleic acid conformations [2–4]. In this regard, interactions of transition metal complexes with nucleic acids have gained attention [5–7].

*Corresponding author. Email: drn_raman@yahoo.co.in

Journal of Coordination Chemistry
ISSN 0095-8972 print/ISSN 1029-0389 online © 2010 Taylor & Francis
DOI: 10.1080/00958972.2010.539212

Metal complexes are useful for design and development of synthetic restriction enzymes, new drugs, DNA footprinting agents, etc. because of their potential to bind DNA *via* a multitude of interactions and to cleave plasmids by virtue of their intrinsic chemical, electrochemical, and photochemical reactivities [8–10]. The nature of the ligand and metal is of paramount importance in the interaction of the complexes with DNA, helping in the design of newer drugs and developing new selective, efficient DNA-recognition and DNA-cleaving agents.

Particularly, copper complexes with aromatic imines have received attention, because of their ability to intercalate between bases of DNA [11, 12], and to participate in catalytic cycles with usual reducing and oxidizing agents in biological media [13, 14]. Recently, the cytotoxicity of some Schiff-base copper(II) complexes toward tumor cells was reported [15]. These complexes are able to transport copper through the cell membrane, trigger oxidative stress inside the cell, and induce apoptosis, targeting mainly the organelles like mitochondria and nuclei, in a process modulated by the imine ligand [16]. Their mechanisms of action involve not only redox activity, with consequent generation of reactive oxygen species (ROS), but also specific interactions with membranes and organelles as delocalized lipophilic cations.

Complexes of 1,10-phenanthroline and 2,2′-bipyridine with transition metals have stimulated research because of their potential application as nonradioactive nucleic acid probes and DNA-cleaving agents [17]. Thus, copper(II) complexes of 1,10-phenanthroline and its derivatives exhibit numerous biological activities, such as antitumor, anti-cancer, antimycobacterial, and antimicrobial activities [17–23]. Considerable attention has focused on the use of phenanthroline complexes as the intercalating agents of DNA [24] and as artificial nucleases [25–28]. However, most studies have focused on mononuclear copper(II) complexes [17–36]. Hence, the present work stems from the interest to design mixed-ligand copper(II) complexes containing biologically important Schiff bases and *N*,*N*-donor heterocyclic bases as DNA groove binders.

2. Experimental

2.1. *Materials and methods*

All reagents and chemicals were procured from Merck products. Solvents used for electrochemical and spectroscopic studies were purified by standard procedures [37]. DNA was purchased from Bangalore Genei (India). Agarose (molecular biology grade) and ethidium bromide (EB) were obtained from Sigma (USA). Tris(hydroxymethyl)-aminomethane hydrochloride (Tris-HCl) buffer solution was prepared using deionized, sonicated, triply distilled water.

Carbon, hydrogen, and nitrogen analyses of the complexes were carried out on a CHN analyzer Calrlo Erba 1108, Heraeus. The infrared (IR) spectra (KBr discs) of the samples were recorded on a Perkin-Elmer 783 series FTIR spectrophotometer. Electronic absorption spectra from 200 to 1100 nm were obtained on a Shimadzu UV-1601 spectrophotometer. ^{1}H spectra (300 MHz) of the ligands were recorded on a Bruker Avance DRX 300 FT-NMR spectrometer using $CDCl_3$ as solvent and

tetramethylsilane (TMS) as the internal standard. Fast atom bombardment (FAB) mass spectra of the complexes were recorded on a JEOL SX 102/DA-6000 mass spectrometer/data system using Argon/Xenon (6 kV, 10 mA) as the FAB gas. The accelerating voltage was 10 kV and the spectra were recorded at room temperature using *m*-nitrobenzylalcohol (NBA) as the matrix. The X-band electron paramagnetic resonance (EPR) spectra of the complexes were performed at RT (300 K) and LNT (77 K) using tetracyanoethylene (TCNE) as the g-marker. Molar conductances of 10^{-3} mol L^{-1} solutions of the complexes in *N*,*N*′-dimethylformamide (DMF) were measured at room temperature with a Deepvision Model-601 digital direct reading deluxe conductivity meter. Magnetic susceptibility measurements were carried out by employing the Gouy method at room temperature on powder sample of the complex using $CuSO_4 \cdot 5H_2O$ as the calibrant. Electrochemical measurements were performed on a CHI 620C electrochemical analyzer. The purity of ligands and their complexes was evaluated by column and thin layer chromatography.

2.2. *Synthesis of ligands (L)*

The Schiff bases, 4-[3,4-dimethoxy-benzylidene]-1,5-dimethyl-2-phenyl-1,2-dihydro-pyrazole-3-one (L^1) and 4-[3-hydroxy-4-nitro-benzylidene]-1,5-dimethyl-2-phenyl-1,2-dihydro-pyrazole-3-one (L^2) were prepared as per the method adopted by Raman *et al*. [38].

4-[3,4-Dimethoxy-benzylidene]-1,5-dimethyl-2-phenyl-1,2-dihydro-pyrazole-3-one (L^1); Yield: 82%. M.p. 164°C. IR (KBr): 1660 (cyclic keto group) and 1635 (–CH=N). ^{1}H-NMR ($CDCl_3$): phenyl (multiplet) at 7.0–7.5 δ, –OCH_3 at 3.8 δ, N–CH_3 at 3.0 δ, –C=CH_3– at 2.2 δ, and –CH=N– at 7.9 δ; *m*/*z*: 351; Anal. Calcd for [$C_{20}H_{21}O_3N_3$] (%): C 68.3, H 6.0, N 11.9; Found (%): C 68.0, H 6.0, N 11.5; λ_{max} in EtOH, 37,313 and 27,472 cm^{-1}. The synthesis of ligands is outlined in scheme 1.

4-[3-Hydroxy-4-nitro-benzylidene]-1,5-dimethyl-2-phenyl-1,2-dihydro-pyrazole-3-one (L^2); Yield: 77%. M.p. 178°C. IR (KBr): 1660 (cyclic keto group), 3200–3500 (–OH), and 1641 (–CH=N). ^{1}H-NMR ($CDCl_3$): phenyl (multiplet) at 6.9–7.6 δ, –OCH_3 at 3.8 δ, N–CH_3 at 3.3 δ, –C=CH_3– at 2.3 δ, –OH at 10.1 δ, and –CH=N– at 8.1 δ; *m*/*z*: 352; Anal. Calcd for [$C_{18}H_{16}N_4O_4$] (%): C 62.3, H 4.5, N 15.9; Found (%): C 62.0, H 4.5, N 15.8; λ_{max} in EtOH, 36,101 and 25,706 cm^{-1}.

2.3. *Synthesis of mixed-ligand copper(II) complexes*

2.3.1. Synthesis of [CuL^1(phen)Cl_2] and [CuL^2(phen)Cl_2]. The copper(II) complexes were prepared by mixing the appropriate molar quantity of ligands and copper salt using the following procedure. An ethanolic solution of Schiff base L^1/L^2 (10 mmol) was heated under reflux with the ethanolic solution of copper(II) chloride (10 mmol) for *ca* 3 h. To the above mixture, an ethanolic solution of 1,10-phenanthroline (10 mmol) was added and the reflux was continued for *ca* 1 h. The solid product formed was filtered, washed with ethanol, and dried *in vacuo*. **[CuL^1(phen)Cl_2]:** Yield: 62%. IR (KBr): 1640 (cyclic keto group), 1615 (–CH=N) and 432 (M–N) cm^{-1}. *m*/*z*: 666;

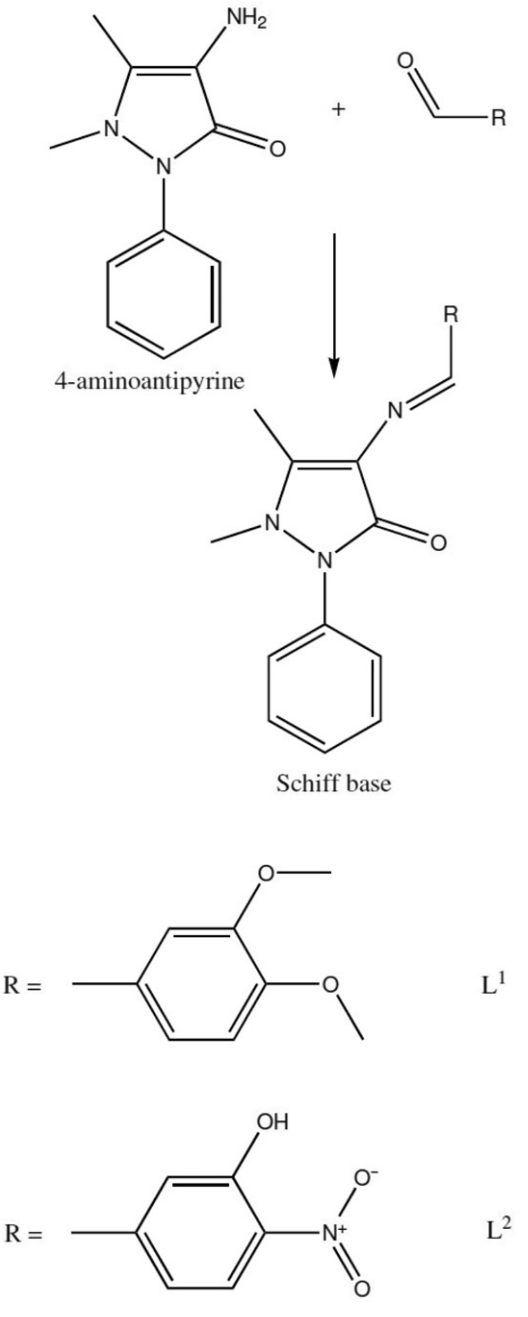

Scheme 1. Outline of the synthesis of L.

Anal. Calcd for $[CuC_{32}H_{29}O_3N_5Cl_2]$ (%): M 9.5, C 57.7, H 4.3, N, 10.5; Found (%): M 9.2, C 55.5, H 4.3, N 10.1; λ_M 10^{-3} (Ω^{-1} cm^2 mol^{-1}), 14. μ_{eff} (BM), 1.74. λ_{max} in DMF, 42553, 32679, 27397, and 13586 cm^{-1}. **[CuL^2(phen)Cl$_2$]:** Yield: 54%. IR (KBr): 1645 (cyclic keto group), 1610 (–CH=N), 3200–3500 (–OH) and 425 (M–N) cm^{-1}. *m*/*z*: 667;

Anal. Calcd for $[CuC_{30}H_{24}N_6O_4Cl_2]$ (%): M 9.5, C 54.0, H 3.6, N 12.6; Found (%): M 9.1, C 53.6, H 3.6, N 12.4; λ_M 10^{-3} (Ω^{-1} cm^2 mol^{-1}), 10. μ_{eff} (BM), 1.70. λ_{max} in DMF, 38,167, 27,472, and 14,492 cm^{-1}.

2.3.2. Synthesis of $[CuL^1(bipy)Cl_2]$ and $[CuL^2(bipy)Cl_2]$. An ethanolic solution of Schiff base L^1/L^2 (10 mmol) was heated under reflux with the ethanolic solution of copper chloride (10 mmol) for *ca* 3 h. To the above mixture, an ethanolic solution of 2,2′-bipyridine (10 mmol) was added and the reflux was continued for *ca* 1 h. The green product formed was filtered, washed with ethanol and dried *in vacuo*. **$[CuL^1(bipy)Cl_2]$:** Yield: 65%. IR (KBr): 1644 (cyclic keto group), 1608 (–CH=N) and 422 (M–N) cm^{-1}. *m*/*z*: 642; Anal. Calcd for $[CuC_{30}H_{29}O_3N_5Cl_2]$ (%): M 9.9, C 56.1, H 4.5, N 10.9; Found (%): M 9.7, C 56.0, H 4.5, N 10.4; λ_M 10^{-3} (Ω^{-1} cm^2 mol^{-1}), 8. μ_{eff} (BM), 1.79. λ_{max} in DMF, 39370, 27624, and 13005 cm^{-1}. **$[CuL^2(bipy)Cl_2]$:** Yield: 59%. IR (KBr): 1638 (cyclic keto group), 1617 (–CH=N), 3200–3500 (–OH), and 425 (M–N) cm^{-1}. *m*/*z*: 642; Anal. Calcd for $[CuC_{28}H_{24}N_6O_4Cl_2]$ (%): M 9.8, C 52.3, H 3.7, N 13.0; Found (%): M 9.5, C 51.6, H 3.7, N 12.7; λ_M 10^{-3} (Ω^{-1} cm^2 mol^{-1}), 16. μ_{eff} (BM), 1.74. λ_{max} in DMF, 42,553, 26,954, and 14,124 cm^{-1}.

2.3.3. Synthesis of $[Cu(L^1)_2Cl_2]$and $[Cu(L^2)_2Cl_2]$. An ethanolic solution of Schiff base L^1/L^2 (20 mmol) was heated under reflux with the ethanolic solution of copper chloride (10 mmol) for *ca* 5 h. The brown solid product formed was filtered, washed with ethanol and dried *in vacuo*. **$[Cu(L^1)_2Cl_2]$:** Yield: 48%. IR (KBr): 1643 (cyclic keto group), 1612 (–CH=N), and 439 (M–N) cm^{-1}. *m*/*z*: 837; Anal. Calcd for $[CuC_{40}H_{42}O_6N_6Cl_2]$ (%): M 7.5, C 57.3, H 5.0, N 10.0; Found (%): M 7.2, C 57.0, H 5.0, N 9.8; λ_M 10^{-3} (Ω^{-1} cm^2 mol^{-1}), 12. μ_{eff} (BM), 1.72. λ_{max} in DMF, 42553, 26041, and 13123 cm^{-1}. **$[Cu(L^2)_2Cl_2]$:** Yield: 59%. IR (KBr): 1642 (cyclic keto group), 1614 (–CH=N), 3200–3500 (–OH), and 442 (M–N) cm^{-1}. *m*/*z*: 839; Anal. Calcd for $[CuC_{36}H_{32}N_8O_8Cl_2]$ (%): M 7.5, C 51.5, H 3.8, N 13.3; Found (%): M 7.1, C 51.0, H 3.7, N 13.1; λ_M 10^{-3} (Ω^{-1} cm^2 mol^{-1}), 11. μ_{eff} (BM), 1.73. λ_{max} in DMF, 40,983, 26,109, and 13,812 cm^{-1}.

2.4. *DNA-binding and cleavage experiments*

All experiments involving interaction of the complexes with calf thymus (CT) DNA were carried out in Tris-HCl buffer (50 mmol Tris-HCl, pH 7.2) containing 5% DMF at room temperature. A solution of CT DNA in the buffer gave a ratio of UV absorbance at 260 and 280 nm of about 1.8–1.9 : 1, indicating that the CT DNA was sufficiently free from protein [39]. The CT DNA concentration per nucleotide was determined by absorption spectroscopy using the molar absorption coefficient of 6600 mol L^{-1} cm^{-1} at 260 nm [40].

2.4.1. Absorption spectroscopic studies. Absorption titration experiments were performed by maintaining the copper complex concentration at 50 μmol L^{-1} while varying the concentration of CT DNA within 40–400 μmol L^{-1}. While measuring the absorption spectra, equal quantity of CT DNA was added to both the complex solution and the reference solution to eliminate the absorbance of CT DNA. From the absorption data,

the intrinsic binding constant K_b was determined from a plot of [DNA]/($\varepsilon_a - \varepsilon_f$) *versus* [DNA] using equation (1)

$$[\text{DNA}]/(\varepsilon_a - \varepsilon_f) = [\text{DNA}]/(\varepsilon_b - \varepsilon_f) + [K_b(\varepsilon_b - \varepsilon_f)]^{-1}, \quad (1)$$

where [DNA] is the concentration of CT DNA in base pairs. The apparent absorption coefficients ε_a, ε_f, and ε_b correspond to A_{obsd}/[Cu], the extinction coefficient for the free Cu(II) complex, and extinction coefficient for the Cu(II) complex in the fully bound form, respectively [41]. K_b is given by the ratio of slope to the intercept.

2.4.2. Electrochemical methods. Cyclic voltammetry (CV) and differential pulse voltammetry were performed on a CHI 620C electrochemical analyzer with a three electrode system of gold as the working electrode, a platinum wire as auxiliary electrode, and Ag/AgCl as the reference electrode. Solutions were deoxygenated by purging with N_2 prior to measurements. The freshly polished gold electrode was modified by transferring a droplet of 2 μL of 3×10^{-3} mol L^{-1} of CT DNA solution onto the surface, followed by air drying. Then the electrode was rinsed with distilled water. Thus, a CT DNA-modified gold electrode was obtained.

2.4.3. Viscosity measurements. Viscosity experiments were carried on an Ostwald viscometer, immersed in a thermostated water-bath maintained at 30.0 ± 0.1°C. CT DNA samples of approximately 0.5 mmol were prepared by sonication in order to minimize complexities arising from CT DNA flexibility [42]. Flow time was measured with a digital stopwatch three times for each sample and an average flow time was calculated. Data are presented as $(\eta/\eta^0)^{1/3}$ *versus* the concentration of the copper(II) complexes, where η is the viscosity of CT DNA solution in the presence of complex and η^0 is the viscosity of CT DNA solution in the absence of complex. Viscosity values were calculated after correcting the flow time of buffer alone (t_0), $\eta = (t - t_0)/t_0$ [43].

2.4.4. DNA cleavage study. The extent of cleavage of supercoiled (SC) pUC19 DNA (33.3 μmol L^{-1}, 0.2 μg) to its nicked circular (NC) form was determined by agarose gel electrophoresis in 50 mmol Tris-HCl buffer (pH 7.2) containing 50 mmol NaCl. For photo-induced DNA cleavage studies, the reactions were carried out under illumination using UV sources at 360 nm. After exposure to light, each sample was incubated for 1 h at 37°C and analyzed for the photo-cleaved products using gel electrophoresis as discussed below. The inhibition reactions for the "chemical nuclease" reactions were carried out in the dark by adding reagents (distamycin 50 μmol L^{-1} and DMSO 4 μL) prior to the addition of each complex and the reducing agent 3-mercaptopropionic acid (MPA). Inhibition reactions for photo-induced DNA were carried out at 360 nm using NaN_3 100 μmol L^{-1} and DMSO 4 μL prior to the addition of each complex. For the D_2O experiment, the solvent (D_2O) was used for dilution of the sample to 18 μL; the samples after incubation for 1 h at 37°C in a dark chamber were added to the loading buffer containing 25% bromophenol blue, 0.25% xylene cyanol, 30% glycerol (3 μL), and the solution was finally loaded on 0.8% agarose gel containing 1 μg mL^{-1} EB. Electrophoresis was carried out in a dark chamber for 3 h at 50 V in Tris-acetate–EDTA buffer. Bands were visualized by UV light and photographed.

2.5. *Antimicrobial activity*

The *in vitro* biological screening effects of the investigated compounds were tested against the bacteria *Salmonella typhi*, *Staphylococcus aureus*, *Escherichia coli*, and *Bacillus subtilis* by the disc diffusion method, using agar nutrient as the medium and streptomycin as the standard. The antifungal activities of the compounds were evaluated by the disc diffusion method against the fungi, namely *Aspergillus niger*, *Aspergillus flavus*, *Candida Albicans*, and *Rhizoctonia bataicola* cultured on potato dextrose agar as medium and nystatin as the standard. The stock solution (10^{-2} mol L^{-1}) was prepared by dissolving the compounds in DMSO and the solutions were serially diluted in order to find the minimum inhibitory concentration (MIC). In a typical procedure [44], the disc was filled with the test solution using a micropipette and the plate was incubated, 24 h for bacteria and 72 h for fungi, at 35°C. During this period, the test solution diffused and the growth of the inoculated microorganisms was affected. The inhibition zone was developed, at which the concentration was noted.

3. Results and discussion

The ligands and their copper(II) complexes are stable in air. The ligands are soluble in common organic solvents and complexes are soluble only in DMF and DMSO. The elemental analyses data of the synthesized ligands and their copper complexes, shown in Section 2, are in good agreement with the presented formulae. The physico-chemical and spectroscopic studies of synthesized complexes indicate the formation of mono-metallic complexes $[CuLXCl_2]$, where L = primary ligands and X = co-ligands such as 1,10-phenanthroline, 2,2′-bipyridine. The complexes show low conductance values which support their non-electrolytic nature and are consistent with related metal complexes [45]. The absence of chloride ion is evident from Volhard's test. The magnetic moment values of the complexes indicate the presence of one unpaired electron.

3.1. *Mass spectra*

The FAB-mass spectra of synthesized ligands and their copper complexes show molecular ion peaks which confirm the proposed formula. The mass spectrum of L^1 shows the molecular ion peak at m/z 351 corresponding to $[C_{20}H_{21}O_3N_3]^+$. The mass spectrum of $[CuL^1(phen)Cl_2]$, that is $[Cu(C_{20}H_{21}O_3N_3)(C_{12}H_8N_2Cl_2)]$ shows m/z 666. The strongest peak (base beak) at m/z 351 represents the stable ($C_{20}H_{21}O_3N_3$) species, L^1. Moreover, the spectrum exhibits the fragments at m/z 595, 244, and 180 corresponding to $[CuC_{32}H_{29}O_3N_5]^+$, $[CuC_{12}H_8N_2]^+$, and $[C_{12}H_8N_2]^+$, respectively. These are due to the fragment remaining after the removal of two chlorides, the presence of copper phen and phen, respectively. Similarly, the other fragments are also in good agreement with the proposed structure of the complex. Thus, mass spectral data confirm the stoichiometry of the complexes as $[CuLXCl_2]/[CuL_2Cl_2]$ (where L = ligand, L^1/L^2; X = phen/bipy) type. The mass spectral data of other complexes also support the above stoichiometry. This stoichiometry is further supported by the elemental data which are in close agreement with the values calculated from molecular formulae

assigned to these complexes. Thus, the mass spectral data reinforce the conclusion drawn from the analytical and conductance values.

3.2. *IR spectra*

Determination of the coordinating atoms was made on the basis of comparison of IR spectra of the ligands and complexes. The spectra of the free Schiff bases show a strong band at 1660 cm^{-1}, characteristic for the cyclic keto group present in the pyrazolone ring [46, 47], which is shifted to lower frequencies upon complexation. Bands at 1635 and 1641 cm^{-1} in the free ligands are due to azomethine group, which is shifted to lower frequencies in the spectra of the complexes (1615–1605 cm^{-1}) indicating the involvement of –C=N nitrogen in coordination to the metal [48] and lowering of $\nu_{(C=N)}$ in the complexes (1615–1605 cm^{-1}) as compared to the phenanthroline and bipyridine (1630 cm^{-1}) [49] due to the reduction of double bond character of carbon–nitrogen bond. This indicates that the metal ion is coordinated by the nitrogens of 1,10-phenanthroline [50] and 2,2′-bipyridine. All the complexes show bands at 1090–1100 and 700–750 cm^{-1}, assigned to phenyl ring vibrations. Assignment of the proposed coordination sites is further supported by the appearance of medium bands at 400–450 cm^{-1}, attributed to ν_{M-N} [51].

3.3. *NMR spectra*

The ^{1}H-NMR spectrum of L^1 at room temperature in $CDCl_3$ shows the following signals: –N–CH_3, –OCH_3, and =C–CH_3 appear as singlets at 3.0 δ, 3.8 δ, and 2.2 δ, respectively; the aromatic phenyl ring appears as the multiplet around 7.0–7.5 δ. In pyrazolone, azomethine proton appears as a singlet at 7.9 δ. ^{1}H-NMR study reinforces the conclusions drawn from IR spectra.

3.4. *Electronic absorption spectra and magnetic measurements*

Absorption band assignments and proposed geometry of the complexes are given in table 1. In general, spectra of the six coordinate Cu(II) complexes exhibit a broad band, frequently with shoulder(s) in the visible region, 10,000–15,000 cm^{-1}. The band is assigned to $^2E_g \rightarrow {}^2T_{2g}$ transition [52]. These states arise due to the splitting of ^{2}D state of Cu(II) ion in a regular octahedral field. The electronic absorption spectra of the present Cu(II) chelates show bands at *ca* 13,005–14,492 cm^{-1}, presumably due to $^2E_g \rightarrow {}^2T_{2g}$ transition for distorted octahedral structure. A shoulder which appears near 26,000 cm^{-1} (table 1) is attributed to the $\pi \rightarrow$ copper(II) ligand-to-metal charge-transfer (LMCT) transition [53]. The high-intensity bands observed at lower wavelength (38,000–40,000 cm^{-1}) are due to π–π^* transitions of HC=N and LMCT transitions. The charge transfer may be from the p orbital of coordinated ketonic oxygen or nitrogen to the vacant d orbitals of copper(II) [54]. The magnetic moment values of the complexes indicate the presence of one unpaired electron.

Table 1. Electronic absorption spectral data of the synthesized compounds at 300 K.

S. No.	Compound	Solvent	Absorption (cm^{-1})	Band assignment	Geometry
1	L^1	EtOH	37,313	INCT	–
			27,472	INCT	
2	L^2	EtOH	36,101	INCT	–
			25,706	INCT	
3	$[CuL^1(Phen)Cl_2]$	DMF	42,553	INCT	Distorted octahedral
			32,679	INCT	
			27,397	INCT	
			13,586	$^2E_g \rightarrow {}^2T_{2g}$	
4	$[CuL^1(bipy)Cl_2]$	DMF	39,370	INCT	Distorted octahedral
			27,624	INCT	
			13,005	$^2E_g \rightarrow {}^2T_{2g}$	
5	$[CuL^1_2Cl_2]$	DMF	42,553	INCT	Distorted octahedral
			26,041	INCT	
			13,123	$^2E_g \rightarrow {}^2T_{2g}$	
6	$[CuL^2(phen)Cl_2]$	DMF	38,167	INCT	Distorted octahedral
			27,472	INCT	
			14,492	$^2E_g \rightarrow {}^2T_{2g}$	
7	$[CuL^2(bipy)Cl_2]$	DMF	42,553	INCT	Distorted octahedral
			26,954	INCT	
			14,124	$^2E_g \rightarrow {}^2T_{2g}$	
8	$[CuL^2_2Cl_2]$	DMF	40,983	INCT	Distorted octahedral
			26,109	INCT	
			13,812	$^2E_g \rightarrow {}^2T_{2g}$	

3.5. *EPR spectra*

The X-band EPR spectrum of polycrystalline copper complex in DMSO recorded at room temperature exhibits absorption with axial symmetry and partial resolution of a hyperfine structure. In DMSO frozen solution, the hyperfine structure is well-resolved and presents four lines in the $g_\parallel$ region which are assigned to the interaction of the paramagnetic electron with the Cu(II) nucleus ($I = 3/2$).

Typical spectra of $[CuL^1(phen)Cl_2]$ are shown in figure S1 (Supplementary material) and spin Hamiltonian parameters of the L^1 complexes are reported in table 2. The $g_\parallel$ values are greater than the corresponding $g_\perp$ values indicating the unpaired electron occupies the $d_{x^2-y^2}$ orbital [55, 56].

The bonding coefficients (in-plane π-bonding β^2, in-plane σ-bonding α^2, and out-of plane π-bonding γ^2) were calculated using simplified M.O. theory and the results are summarized in table 3; $\alpha^2 = 1.0$ indicates complete ionic character and $\alpha^2 = 0.5$ denotes 100% covalent bonding, with assumption of negligible overlap integral.

The α^2 and β^2 values indicate more interaction to the in-plane π-bonding than in-plane σ-bonding whereas the in-plane π-bonding is almost ionic. The lower value of α^2 compared to β^2 indicates that the in-plane σ-bonding is more covalent than in-plane π-bonding. These data are in accord with reported values [57]. The observed exchange interaction term G indicates that the exchange interaction between Cu–Cu nuclei is not significant.

$$G = (g_\parallel - 2.0023)/(g_\perp - 2.0023).$$

The observed order for orbital reduction factor values ($K_\parallel > K_\perp$) for the copper complexes suggests that out-of plane π-bonding is significant. Based on these

Table 2. Spin Hamiltonian parameters of copper complexes in DMSO at 300 and 77 K.

	Hyperfine constant $\times 10^{-4}\,cm^{-1}$					
Complex	$A_\perp$	$A_\parallel$	A_{iso}	$g_\parallel$	$g_\perp$	g_{iso}
$[CuL^1(phen)Cl_2]$	24	115	65.5	2.36	2.06	2.14
$[CuL^1(bipy)Cl_2]$	26	121	70.1	2.38	2.05	2.13
$[CuL^1_2Cl_2]$	28	111	66.4	2.37	2.04	2.12

Table 3. Bonding parameters of copper complexes in DMSO.

Complex	α^2	β^2	γ^2	G	$K_\parallel$	$K_\perp$
$[CuL^1(phen)Cl_2]$	0.74	0.99	0.63	6.1	0.73	0.47
$[CuL^1(bipy)Cl_2]$	0.77	1.03	0.45	7.9	0.79	0.35
$[CuL^1_2Cl_2]$	0.73	0.99	0.40	9.7	0.72	0.30

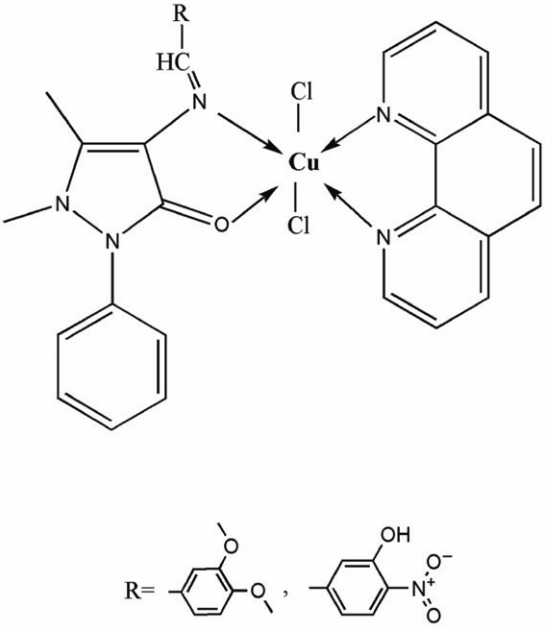

Figure 1. Proposed structure of the mixed-ligand copper complexes.

observations, distorted octahedral geometry is proposed for the complexes. EPR of the copper(II) complexes provides support to the conclusion obtained on the basis of electronic spectrum and magnetic moment values.

The proposed structure of the Schiff base mixed-ligand 1,10-phenanthroline copper(II) complexes is given in figure 1.

Table 4. Absorption spectral properties of synthesized complexes with DNA.

S. No.	Complexes	λ_{max} Free	λ_{max} Bound	$\Delta\lambda$ (nm)	Hypochromicity H (%)	$K_b \times 10^5$ (mol L^{-1})
1	$[CuL^1(phen)Cl_2]$	384	378.0	6.0	7.4	2.5 ± 0.03
2	$[CuL^1(bipy)Cl_2]$	371	367.5	3.5	5.8	1.5 ± 0.05
3	$[CuL^1_2Cl_2]$	365	369.5	4.5	3.9	0.6 ± 0.02
4	$[CuL^2(phen)Cl_2]$	383	376.5	6.5	8.7	3.9 ± 0.04
5	$[CuL^2(bipy)Cl_2]$	362	356.5	5.5	6.4	2.0 ± 0.08
6	$[CuL^2_2Cl_2]$	364	366.5	2.5	5.2	1.0 ± 0.01

3.6. *DNA-binding experiments*

3.6.1. Absorption spectroscopic studies. The binding of the copper complexes to the CT DNA has been studied by electronic absorption. Electronic absorption spectra of $[CuL^1(phen)Cl_2]$ and $[CuL^2(phen)Cl_2]$ in the absence and presence of CT-DNA in 5 mmol Tris-HCl, 50 mmol NaCl, pH 7.2 buffer are shown in figures S2 and S3, respectively (Supplementary material).

In the UV region, intense absorptions with maxima of 365 nm for $[CuL^1(phen)Cl_2]$, 362 nm for $[CuL^1(bipy)Cl_2]$, 384 nm for $[CuL^1_2Cl_2]$, 364 nm for $[CuL^2(phen)Cl_2]$, 371 nm for $[CuL^2(bipy)Cl_2]$, and 383 nm for $[CuL^2_2Cl_2]$ are attributed to intraligand π–π^* transitions. Increasing concentration of CT-DNA results in hypochromism, and red-shift in the UV-Vis spectrum of $[CuL^1(phen)Cl_2]$. These spectral characteristics suggest that the π^* orbital of the intercalated ligand couples with the π orbital of base pairs, thus decreasing the π–π^* transition energy and further resulting in the red shift. Coupling of the π orbital partially filled by electrons decreases the transition probabilities and concomitantly results in hypochromism. A similar type of binding mode is observed for other complexes with CT-DNA (table 4).

In order to compare the binding strength of the complexes with CT-DNA, the intrinsic binding constants K_b are obtained by monitoring the changes in absorbance with increasing concentration of DNA. K_b is obtained from the ratio of the slope to the intercept from plots of $[DNA]/(\varepsilon_a - \varepsilon_f)$ *versus* [DNA]. The K_b values are on the order of 10^5.

The intrinsic binding constant of the synthesized complexes is in the following order: $[CuL^2(phen)Cl_2] > [CuL^1(phen)Cl_2] > [CuL^2(bipy)Cl_2] > [CuL^1(bipy)Cl_2] > [CuL^2_2Cl_2] > [CuL^1_2Cl_2]$. The high K_b value for $[CuL^2(phen)Cl_2]$ in comparison to its bpy analogue is due to the presence of extended planar structure of the phen ligand which facilitates the groove binding/stacking with the base pairs. The $[CuL^1_2Cl_2]$ complex without a planar moiety does not show any apparent binding to DNA.

Thus, the above order indicates that planarity and flexible extended conjugation of the ligands play an important role in binding strength of the complexes with CT-DNA. The complexes have moderate binding compared to other copper and ruthenium complexes but smaller than classical intercalators and metallointercalators whose binding constants are in the order of 10^7 [58–61].

3.6.2. Electrochemical studies. The application of CV to study binding of metal complexes to DNA is a useful complement. The typical cyclic voltammogram of

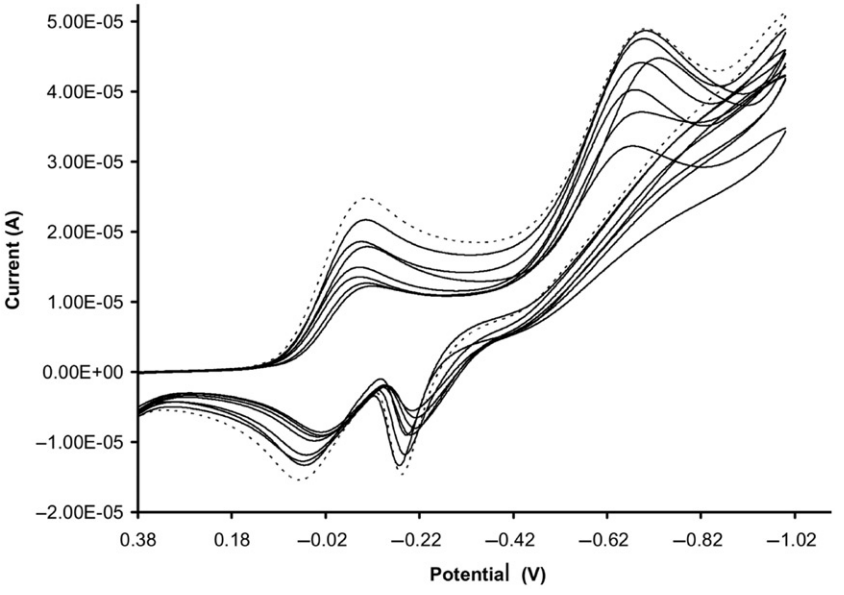

Figure 2. Cyclic voltammogram of $[CuL^1(phen)Cl_2]$ both in the absence (- - -) and presence (——) of different concentrations of DNA.

$[CuL^1(phen)Cl_2]$ in the absence and presence of varying amount of [DNA] is shown in figure 2. The cathode and anode peak currents decrease in the presence of DNA. The decrease in current may be attributed to molecules bound to DNA [62].

In the absence of DNA, first redox couple cathodic peak appears at −0.106 V for Cu(III) → Cu(II) and second redox couple cathodic peak appears at −0.708 V for Cu(II) → Cu(I). These two redox couples ratio of I_{pc}/I_{pa} is approximately unity, indicating that the reaction of the complex on the working electrode surface is quasi-reversible. In the incremental addition of DNA to the complex, the second redox couple causes a negative shift in $E_{1/2}$ of 60 mV and a decrease in ΔE_p of 112 mV. The I_{pc}/I_{pa} values decrease in the presence of DNA in the first redox couple (Cu(III) → Cu(II)) and also in the second (Cu(II) → Cu(I)). The peak potentials, E_{pc} and E_{pa}, as well as $E_{1/2}$, shift to more negative potential. The changes of peak currents and shifts of potential are observed upon addition of CT DNA, indicating that all the copper complexes have DNA-binding affinity. The results are similar to the spectroscopic and viscosity data of the complexes in the presence of DNA.

Differential pulse voltammograms of $[CuL^1(phen)Cl_2]$ and $[CuL^1(bipy)Cl_2]$ in the absence and presence of varying amount of [DNA] are given in figures S4 and S5 (Supplementary material). Increase in the concentration of DNA causes a negative potential shift along with significant increase in current intensity. The shift in potential is related to the ratio of binding constant:

$$E^{o}_{b'} - E^{o}_{f'} = 0.0591 \log(K_+/K_{2+}),$$

where $E^{o}_{b'}$ and $E^{o}_{f'}$ are formal potentials of the Cu(II)/Cu(I) complex couple in the bound and free form, respectively. The ratio of K_+/K_{2+} for DNA-binding

Table 5. Electrochemical parameters for the interaction of DNA with Cu(II) complexes.

			$E_{1/2}$ (V)		ΔE_p (V)			
SI. No.	Complexes	Redox couple	Free	Bound	Free	Bound	k[red]/k[oxd]	I_{pc}/I_{pa}
1	$[CuL^1(Phen)Cl_2]$	Cu(III)/Cu(II)	−0.028	−0.089	0.156	0.180	0.79	1.9
		Cu(II)/Cu(I)	−0.441	−0.435	0.534	0.646	1.40	0.4
2	$[CuL^1(bipy)Cl_2]$	Cu(III)/Cu(II)	0.005	−0.002	−0.086	0.024	2.40	1.5
		Cu(II)/Cu(I)	–	–	–	–	0.75	–
3	$[CuL^1_2Cl_2]$	Cu(III)/Cu(II)	−0.569	−0.544	0.097	0.074	0.72	1.4
4	$[CuL^2(phen)Cl_2]$	Cu(III)/Cu(II)	−0.439	−0.438	0.383	0.384	–	0.75
		Cu(II)/Cu(I)	−0.600	−0.495	0.278	0.425	0.84	1.50
5	$[CuL^2(bipy)Cl_2]$	Cu(III)/Cu(II)	−0.569	−0.544	0.097	0.074	0.72	1.40
6	$[CuL^2_2Cl_2]$	Cu(II)/Cu(I)	−0.958	−0.907	0.013	0.028	0.80	0.92

of Cu(II)/Cu(I) complexes is greater than unity (table 5), indicating that the binding of Cu(II) complex to DNA is small compared to that of the Cu(I) complex. The electrochemical results indicate preferential stabilization of Cu(II) form over Cu(I) form on binding to DNA.

3.6.3. Viscosity measurements. To further explore the binding mode of the copper(II) complexes, viscosity measurements on solutions of CT DNA incubated with the complexes are carried out. Since the relative specific viscosity of DNA reflects the increase in contour length associated with the separation of DNA base pairs caused by intercalation, classical intercalators such as EB can cause a significant increase in viscosity of DNA solutions. In contrast, a partial and/or non-classical intercalation of the ligand can bend or kink DNA resulting in a decrease in its effective length with a concomitant increase in its viscosity [63]. The plots of relative specific viscosities *versus* [Complex]/[DNA] are shown in figure 3. The viscosity of DNA is increased on increasing the concentration of the complexes. However, the increase in the viscosity is much less than intercalators like EB in the same DNA concentration range [64, 65]. This supports the above studies which suggest that the complexes interact with DNA *via* partial intercalation between DNA base pairs, similar to the interaction of other copper complexes with DNA [35].

3.7. *Nuclease activity of complexes and mechanistic investigations*

3.7.1. Oxidative cleavage of DNA. DNA cleavage by ligand alone is inactive in the presence or absence of external agents. Thus, the metal is important for observing chemical nuclease activity. The oxidative cleavage of pUC19 DNA (figure S6, Supplementary material) in the presence of an external reducing agent like MPA (5 mmol) has been studied by gel electrophoresis using SC pUC19 DNA (0.2 μg, 33.3 μmol L^{-1}) in 5 mmol Tris-HCl/ 50 mmol NaCl buffer (14 μL, pH 7.2) and the complexes (50 μmol L^{-1}). Control experiments using MPA or the synthesized complexes alone show apparent cleavage of SC DNA under dark condition. This suggests that the synthesized complexes are able to bind DNA.

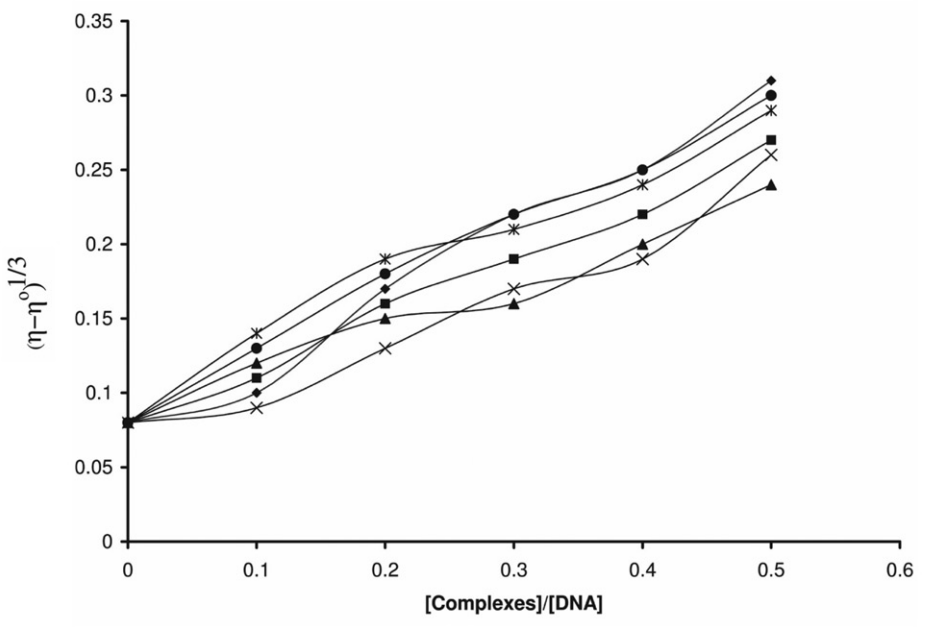

Figure 3. The effect of $[CuL^1(phen)Cl_2]$ (▲), $[CuL^1(bipy)Cl_2]$ (✱), $[CuL^1_2Cl_2]$ (♦), $[CuL^2(phen)Cl_2]$, (●), $[CuL^2(bipy)Cl_2]$ (×), and $[CuL^2_2Cl_2]$ (■) on the viscosity of DNA.

To determine the groove selectivity of the complexes, control experiments are performed using minor groove binder distamycin. The addition of distamycin does not inhibit the cleavage for $[CuL^1(phen)Cl_2]$ (lane 1), indicating major groove binding for the synthesized complexes with DNA. On adding DMSO (hydroxyl radical scavenger), no inhibition of DNA cleavage is observed, indicating hydroxyl radical is not involved in the cleavage process (lane 2). Addition of sodium azide (singlet oxygen scavenger) decreases the cleavage efficiencies revealing that $^1O_2$ is not the activated oxygen intermediate responsible for cleavage (lane 3). The slight suppression of cleavage may be ascribed to the affinity of sodium azide for transition metals [66]. Addition of superoxide dismutase (superoxide scavenger) to the reaction mixture shows no significant quenching of cleavage revealing that superoxide is also not the active species (not shown) [66]. Thus no freely diffusible oxygen intermediate or hydroxyl radical is involved in the strand scission and hence a simple diffusible radical is ruled out. We propose that the active species is either a copper-oxene or a copper-coordinated hydroxyl radical which are directly responsible for initiating the cleavage reaction [67, 68]. The reactive species is tightly coordinated to copper(II), thus preventing them from being deactivated by radical inhibitors. A copper-oxene or a resonance hybrid of a copper hydroxyl radical and a putative copper(III)-oxo species, which generates a deoxyribose-centered radical by C-1 hydrogen abstraction, is the species responsible for DNA cleavage [69].

3.7.2. Photocleavage. Irradiation of pUC19 DNA containing the Cu(II) complexes is carried out in the presence and absence of various "inhibitors" using

Table 6. MIC of the synthesized compounds against the growth of four fungi (mg mL^{-1}).

S. No.	Compound	*A. niger*	*A. flavus*	*C. albicans*	*R. bataicola*
1	L^1	82	71	62	60
2	L^2	73	67	60	77
4	$[CuL^1(phen)Cl_2]$	39	53	49	36
5	$[CuL^1(bipy)Cl_2]$	26	30	33	31
6	$[CuL^1_2Cl_2]$	37	29	37	39
7	$[CuL^2(phen)Cl_2]$	25	31	40	43
8	$[CuL^2(bipy)Cl_2]$	20	25	27	29
9	$[CuL^2_2Cl_2]$	31	47	52	55
10	Nystatin	10	8	14	12

gel electrophoresis. All the complexes cleave the DNA from its SC to NC form even in the absence of inhibitors on irradiation with UV light at 360 nm. In the presence of inhibitors D_2O and DMSO are used to assess the possibility that photoactivated change involves formation of singlet oxygen and hydroxyl radical, respectively, which are responsible for cleavage of DNA. Singlet oxygen is expected to induce more strand scission in D_2O than in H_2O, due to its longer lifetime in D_2O. In figure S7 (Supplementary material), lane 3, obvious inhibitions are observed in the presence of sodium azide, indicating that singlet oxygen is likely to be the reactive species. The hydroxyl radical scavenger DMSO also fails to inhibit cleavage, which argues against the participation of hydroxyl radical (lane 2). These results indicate that, besides the presence of inhibitors, the complexes show cleavage activity upon irradiation with UV light at 360 nm.

The proposed mechanistic pathway involved for photo-induced cleavage of SC-DNA by complex is shown below:

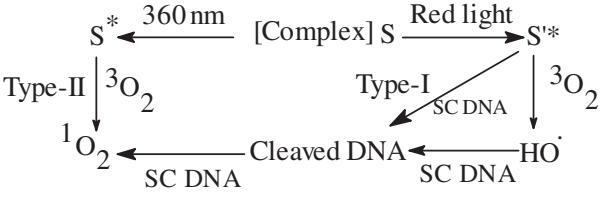

3.8. *Screening for antibacterial and antifungal activities*

For *in vitro* antimicrobial activity, the investigated compounds were tested against bacteria and fungi. The MIC values of the investigated compounds are summarized in tables 6 and 7. A comparative study of the ligands and their complexes (MIC values) indicates that complexes exhibit higher antimicrobial activity than the free ligands. From the MIC values, $[CuL(bipy)Cl_2]$ complexes are found to be more potent than other investigated complexes. Increased activity on metal chelation can be explained on the basis of chelation theory [70, 71]. Besides this, the complexes may also indulge in the formation of hydrogen bond interactions through coordinated anions and azomethine with the active centers of cell constituents. The factors capable of increasing lipophilic nature are expected to enhance the antimicrobial property. While chelation is not the

Table 7. MIC of the synthesized compounds against the growth of four bacteria ($mg\,mL^{-1}$).

S. No.	Compound	*E. coli*	*Sa. typhi*	*St. aureus*	*B. subtilis*
1	L^1	58	69	65	73
2	L^2	61	65	63	70
4	$[CuL^1(phen)Cl_2]$	19	21	26	31
5	$[CuL^1(bipy)Cl_2]$	24	25	17	21
6	$[CuL^1_2Cl_2]$	31	37	39	31
7	$[CuL^2(phen)Cl_2]$	15	19	19	35
8	$[CuL^2(bipy)Cl_2]$	20	21	25	16
9	$[CuL^2_2Cl_2]$	31	32	35	26
10	Streptomycin	10	12	14	13

only criterion for antimicrobial activity, it is an intricate blend of several contributions such as the nature of the metal ion and the ligand, the geometry of the metal complex, the lipophilicity, the steric, and the pharmacokinetic factors.

4. Conclusion

New mixed ligands and their copper complexes have been designed, synthesized, and characterized. They adopt distorted octahedral geometry around copper. The planarity and flexible extended conjugation of the synthesized ligands have an effect of DNA-binding and cleavage activity of the complexes. Mechanistic investigations show major groove binding for the copper complexes with DNA. Pathways involving singlet oxygen in the DNA photo-cleavage reactions are proposed from the observation of complete inhibition of the cleavage in the presence of sodium azide and enhancement of cleavage in D_2O. Hydroxyl radical scavengers like DMSO do not show a significant effect in DNA cleavage, suggesting the formation of singlet oxygen as the reactive species in a type-II process. The antimicrobial study reveals that copper complexes have higher activity than the free ligands.

Acknowledgments

The authors express their sincere thanks to the UGC, New Delhi for financial assistance and the Managing Board, Principal and Head of the Department of Chemistry, VHNSN College, Virudhunagar, Tamil Nadu, for their constant encouragement and providing research facilities.

References

[1] C. Liu, S. Yu, D. Li, Z. Liao, X. Sun, H. Xu. *Inorg. Chem.*, **41**, 913 (2002).
[2] P.J. Dandlier, R.E. Holmlin, J.K. Barton. *Science*, **274**, 1465 (1997).
[3] D.B. Hall, R.E. Holmlin, J.K. Barton. *Nature*, **382**, 731 (1996).

[4] E.L. Hegg, J.N. Burstyn. *Coord. Chem. Rev.*, **173**, 133 (1998).
[5] N. Saglam, A. Colak, K. Serbest, S. Dulger, S. Guner, S. Karabocek, A.O. Belduz. *Biometals*, **15**, 357 (2002).
[6] C. Liu, M. Wang, T. Zhang, H. Sun. *Coord. Chem. Rev.*, **248**, 147 (2004).
[7] L. Zhu, Y. Jin, X.Z. Li, J. Wang, D. Kong, H.F. Mi, D.Z. Liao, H.X. Shen. *Inorg. Chim. Acta*, **361**, 29 (2008).
[8] C.N. Sudhamani, H.S. Bhojya Naik, T.R.R. Naik, M.C. Prabhakara. *Spectrochim. Acta*, **72A**, 643 (2009).
[9] N.A.P.K. Maguire, J.F. Wheeler. *Coord. Chem. Rev.*, **211**, 145 (2001).
[10] A.R. Chakravarty. *J. Chem. Sci.*, **118**, 443 (2006).
[11] Y. An, M.L. Tong, L.N. Ji, Z.W. Mao. *J. Chem. Soc., Dalton Trans.*, 2066 (2006).
[12] J. Liu, T.B. Lu, H. Deng, L.N. Ji, L.H. Qu, H. Zhou. *Transition Met. Chem.*, **28**, 116 (2003).
[13] B. Macıias, I. Garcıia, M.V. Villa, J. Borras, M.G. Alvarez, A. Castineiras. *J. Inorg. Biochem.*, **96**, 367 (2003).
[14] A. Amine, Z. Atmani, A.E. Hallaoui, M. Giorgi, M. Pierrot, M. Reglier. *Bioorg. Med. Chem. Lett.*, **12**, 57 (2002).
[15] V.C. Silveira, J.S. Luz, C.C. Oliveira, I. Graziani, M.R. Ciriolo, A.M.C. Ferreira. *J. Inorg. Biochem.*, **102**, 1090 (2008).
[16] G. Filomeni, G. Cerchiaro, A.M.D.C. Ferreira, J.Z. Pedersen, A.D. Martino, G. Rotilio, M.R. Ciriolo. *J. Biol. Chem.*, **282**, 12010 (2007).
[17] D.S. Sigman, D.M. Perrin. *Chem. Rev.*, **93**, 2295 (1993).
[18] F. Schaeffer, S. Rimsky, A. Spassky. *J. Mol. Biol.*, **260**, 523 (1996).
[19] S. Mahadevan, M. Palaniandavar. *Inorg. Chem.*, **37**, 3927 (1998).
[20] M.A. Zoroddu, S. Zanetti, R. Pogni, R. Basosi. *J. Inorg. Biochem.*, **63**, 291 (1996).
[21] J.D. Ranford, P.J. Sadler. *Dalton Trans.*, 3393 (1993).
[22] M. Geraghty, V. Sheridan, M. McCann, M. Devereux, V. McKee. *Polyhedron*, **18**, 2931 (1999).
[23] D.K. Saha, U. Sandbhor, K. Shirisha, S. Padhye, D. Deobagkar, C.E. Anson, A.K. Powell. *Bioorg. Med. Chem. Lett.*, **14**, 3027 (2004).
[24] K.E. Erkkila, D.T. Odom, J.K. Barton. *Chem. Rev.*, **99**, 2777 (1999).
[25] D.S. Sigman. *Biochemistry*, **29**, 9097 (1990).
[26] D.S. Sigman, A. Mazumder, D.M. Perrin. *Chem. Rev.*, **93**, 2295 (1993).
[27] W.K. Pogozelski, T.D. Tullius. *Chem. Rev.*, **98**, 1089 (1998).
[28] S.C. Zhang, Y.G. Zhu, C. Tu, H.Y. Wei, Z. Yang, L.P. Lin, J. Ding, J.F. Zhang, Z.J. Guo. *J. Inorg. Biochem.*, **98**, 2099 (2004).
[29] Z.M. Wang, H.K. Lin, Z.F. Zhou, M. Xu, T.F. Liu, S.R. Zhu, Y.T. Chen. *Bioorg. Med. Chem.*, **9**, 2849 (2001).
[30] S.F. Asad, S. Singh, A. Ahmad, S.M. Hadi. *Toxicol. Lett.*, **131**, 181 (2002).
[31] J.Z. Wu, H. Li, J.G. Zhang, J.H. Xu. *Inorg. Chem. Commun.*, **5**, 71 (2002).
[32] V.G. Vaidyanathan, B.U. Nair. *J. Inorg. Biochem.*, **93**, 271 (2003).
[33] M. Navarro, E.J.C. Fajardo, M.F. Mestre, D. Arrieche, E. Marchan. *J. Inorg. Biochem.*, **97**, 364 (2003).
[34] A.M. Thomas, A.D. Naik, M. Nethaji, A.R. Chakravarty. *Inorg. Chim. Acta*, **357**, 2315 (2004).
[35] T. Hirohama, Y. Kuranuki, E. Ebina, T. Sugizaki, H. Arii, M. Chikira, P.T. Selvi, M. Palaniandavar. *J. Inorg. Biochem.*, **99**, 1205 (2005).
[36] H. Zhang, C.S. Liu, X.H. Bu, M. Yang. *J. Inorg. Biochem.*, **99**, 1119 (2005).
[37] D.D. Perrin, W.L.F. Armarego, D.R. Perrin. *Purification of Laboratory Chemicals*, Pergamon Press, Oxford (1980).
[38] N. Raman, J. Dhaveethu Raja, A. Sakthivel. *Polish J. Chem.*, **81**, 2059 (2007).
[39] J. Marmur. *J. Mol. Biol.*, **3**, 208 (1961).
[40] M.E. Reichmann, S.A. Rice, C.A. Thomas, P. Doty. *J. Am. Chem. Soc.*, **76**, 3047 (1954).
[41] A. Wolfe, G.H. Shimer, T. Meehan. *Biochemistry*, **26**, 6392 (1987).
[42] J.B. Charies, N. Dattagupta, D.M. Crothers. *Biochemistry*, **21**, 3933 (1982).
[43] S. Satyanarayana, J.C. Daborusak, J.B. Charies. *Biochemistry*, **32**, 2573 (1983).
[44] N.M. Aghatabay, Y. Mahmiani, H. Cevik, B. Dulger. *Eur. J. Med. Chem.*, **44**, 365 (2009).
[45] W.J. Geary. *Coord. Chem. Rev.*, **7**, 81 (1971).
[46] B. Kuncheria, P. Indrasenan. *Polyhedron*, **7**, 143 (1988).
[47] A.M. Donia, F.A. El-Saied. *Polyhedron*, **7**, 2149 (1988).
[48] N.P. Priya, S. Arunachalam. *Spectrochim. Acta*, **72A**, 670 (2009).
[49] G.Z. Bai, G.D. Chen, Z.M. Wang, L. Yuan, J.W. Kang, J.Z. Gao. *Chin. J. Inorg. Chem.*, **4**, 32 (1988).
[50] J.J. Zhang, N. Ren, Y.X. Wang, S.L. Xu, R.F. Wang, S.P. Wang. *J. Braz. Chem. Soc.*, **17**, 1355 (2006).
[51] F. Firdaus, K. Fatma, M. Azam. *Spectrochim. Acta*, **72A**, 591 (2009).
[52] A.B.P. Lever. *Inorganic Electronic Spectroscopy*, 2nd Edn, Elsevier, New York (1968).
[53] K.W. Penfield, A.A. Gewirth, E.J. Solomon. *J. Am. Chem. Soc.*, **107**, 4519 (1985).
[54] C.R.K. Rao, P.S. Zacharias. *Polyhedron*, **16**, 1201 (1997).

[55] D.M. Dooley, J. Rawlings, J.H. Dawson, P.J. Stephens, L.E. Andreasson, B.G. Malmstrom, H.B. Gray. *J. Am. Chem. Soc.*, **101**, 5038 (1979).
[56] R.P. John, A. Sreekanth, M.R.P. Kurup, A. Usman, A.R. Ibrahim, H.K. Fun. *Spectrochim. Acta*, **59A**, 1349 (2003).
[57] Y. Song, Q. Wu, P. Yang, N. Luan, L.F. Wang, Y. Liu. *J. Inorg. Biochem.*, **100**, 1685 (2006).
[58] J.G. Liu, B.H. Ye, Q.L. Zhang, X.H. Zou, Q.X. Zhen, X. Thian, L.N. Ji. *J. Biol. Inorg. Chem.*, **5**, 119 (2000).
[59] X.H. Zou, B.H. Ye, Q.L. Zhang, H. Chao, J.G. Liu, L.N. Jim, X.Y. Li. *J. Biol. Inorg. Chem.*, **6**, 143 (2001).
[60] M. Navarro, E.J. Cisneros-Fajardo, A. Sierralta, M. Fernández-Mestre, P. Silva, D. Arrieche, E. Marchán. *J. Biol. Inorg. Chem.*, **8**, 401 (2003).
[61] C. Tu, Y. Shao, N. Gan, Q. Xu, Z. Guo. *Inorg. Chem.*, **43**, 4761 (2004).
[62] B. Peng, H. Chao, B. Sun, H. Li, F. Gao, L.N. Ji. *J. Inorg. Biochem.*, **101**, 404 (2007).
[63] I. Haq, P. Lincoln, D. Suh, B. Norden, B.Z. Chowdhry, J.B. Chaires. *J. Am. Chem. Soc.*, **117**, 4788 (1995).
[64] E.J. Gabbay, R.E. Scofield, C.S. Baxter. *J. Am. Chem. Soc.*, **95**, 7850 (1973).
[65] M. Gonzalez-Alvarez, G. Alzuet, J. Borras, M. Pitie, B. Meunier. *J. Biol. Inorg. Chem.*, **8**, 644 (2003).
[66] D.S. Sigman, M.D. Kuwabara, C.H.B. Chen, T.W. Bruice. *Methods Enzymol.*, **208**, 414 (1991).
[67] E.S.G. Barron, R.H. DeMeio, F. Klemperer. *J. Biol. Chem.*, **112**, 625 (1936).
[68] B. Selvakumar, V. Rajendiran, P.U. Maheswari, H. Stoeckli-Evans, M. Palaniandavar. *J. Inorg. Biochem.*, **100**, 316 (2006).
[69] Z.H. Chohan, H. Pervez, A. Rauf, K.M. Khan, C.T. Supuran. *J. Enzyme Inhib. Med. Chem.*, **19**, 417 (2004).
[70] N. Raman, A. Sakthivel, K. Rajasekaran. *J. Coord. Chem.*, **62**, 1661 (2009).
[71] N. Dharmaraj, P. Viswanathamurthi, K. Natarajan. *Transition Met. Chem.*, **26**, 105 (2001).